2021 43rd Annual International Conference of the
IEEE Engineering in Medicine & Biology Society (EMBC)
Oct 31 - Nov 4, 2021. Virtual Conference

Application of Depth Selectivity Filter to Brain Function Measurement by fNIRS

Keiko Fukuda, Yamato Wakamatsu, Mamiko Fujii

Abstract—**In brain function measurement by fNIRS, reducing the effect of the hemodynamic change on the signal is important. In this study, a depth-selective filter, which is one of the reduction methods, was applied to the brain function measurement and its reduction effect was verified. A Stroop GO/NO-GO task, which is expected to produce a response in the frontal region was used. The experiments showed the effectiveness of reducing the hemodynamic changes with the depth-selective filter. It can be used as a preprocessing tool for estimating the activated region.**

I. Introduction

Functional near-infrared spectroscopy (fNIRS) is a method to calculate the change in hemoglobin concentration by using the wavelength dependence of the absorption coefficient on the oxygenated and the deoxygenated hemoglobin. In the topography method, the light attenuation due to the change in cerebral blood flow according to the brain activity is estimated to occur at the midpoint of light source and detector. [1]. FNIRS is widely used in daily environments due to its portability and noninvasiveness. In particular, the frontal region that controls higher-order emotional and decision-making processes, is expected to be applied to measurement. The easiness of sensor fixing without affected by hair is also an advantage as the measurement.

Here, we consider the characteristics of the blood metabolism in the forehead region. When the oxygen required for brain activity is supplied to the capillaries of the brain tissue, a large influx of arterial blood simultaneously occurs, leading to an increase in oxygenated hemoglobin and a decrease in deoxygenated hemoglobin since the change in the vessel diameter of the capillaries is very small [2]. On the other hand, the hemodynamic changes especially large in the forehead area cause parallel changes in the oxygenated and deoxygenated hemoglobin concentrations in the forehead [3]. Thus, it is necessary to selectively detect and to reduce the superimposed hemodynamic changes for improving measurement accuracy.

For selectively detecting the hemodynamic change, short-distance source-detector (SSD) pairs are used to detect the hemodynamic changes in the superficial layer. SSD pairs are used in several methods, such as multisource detector separation approach [4] and double-density detector arrangement [5]. A depth-selective filter [6] is proposed as one of the suppression ways to detect the hemodynamic changes in the superficial layer.

In this study, we apply the depth-selectivity filter to the measurement of the brain activity using a Stroop GO/NO-GO task [7]. We analyze the effect of the hemodynamic change on the signal according to the brain activity. The purpose of this study is to improve the accuracy of the measured signal and to estimate the brain active reason by fNIRS..

II. Filter Algorithm

The filter algorithm consists of three processes: A forward problem (i.e., preparing the sensitivity), an inverse problem (i.e., obtaining data representation in the inverse space), and a filter process (i.e., removing unwanted signals).

In the forward problem, we considered the case in which the absorption coefficient, μ_a, varies spatially and the reduced scattering coefficient, μ'_s, is homogeneous in a semi-infinite space. Using the Rytov approximation for small perturbations of the absorption coefficient [8], the perturbed fluence, $\Phi(r_s, r_d)$, at the detector position, r_d, is expressed as

$$\Phi(\boldsymbol{r}_s, \boldsymbol{r}_d) = \Phi_0(\boldsymbol{r}_s, \boldsymbol{r}_d)\exp[\Phi_{pert}(\boldsymbol{r}_s, \boldsymbol{r}_d)] , \quad (1)$$

where r_s is the source position and Φ_0 is the unperturbed fluence for the baseline optical properties. $\Phi_{pert}(\boldsymbol{r}_s, \boldsymbol{r}_d)$ is the perturbation caused by a change in the absorption coefficient and is represented by

$$\Phi_{pert}(\boldsymbol{r}_s, \boldsymbol{r}_d) = -\Phi_0(\boldsymbol{r}_s, \boldsymbol{r}_d)^{-1} \int \frac{\delta\mu_a(r)}{D} \Phi_0(\boldsymbol{r}_s, \boldsymbol{r}) G(\boldsymbol{r}, \boldsymbol{r}_d) d\boldsymbol{r}^3 , \quad (2)$$

where $D = 1/(3\mu'_s)$ is the diffusion coefficient, $G(\boldsymbol{r}, \boldsymbol{r}_d)$ is the Green function, and $\delta\mu_a$ is a small perturbation in the absorption coefficient. Here, we implicitly assume that the source is a unit impulse and $\Phi_0(\boldsymbol{r}_s, \boldsymbol{r}_d) = G(\boldsymbol{r}_s, \boldsymbol{r}_d)$. Furthermore, if the spatial variation in μ_a is assumed to be piecewise-constant in the region of interest, the integral of Eq. (2) is discretized into a summation as

$$\Phi_{pert}(\boldsymbol{r}_s, \boldsymbol{r}_d) = -\sum_j \frac{\delta\mu_{a,j}}{D} G(\boldsymbol{r}_s, \boldsymbol{r}_d)^{-1} G(\boldsymbol{r}_s, \boldsymbol{r}) G(\boldsymbol{r}, \boldsymbol{r}_d) \Delta V, \quad (3)$$

where $\delta\mu_{a,j}$ is the perturbation of the absorption coefficient of the j^{th} voxel and V_j denotes the volume of the j^{th} voxel. Accordingly, the i^{th} measured data b_i, observed by the i^{th} SD pair, are expressed according to the sensitivity $A_{i,j}$, and the elements of the absorption-coefficient perturbation x_j, as

*Research supported by Grants-in-Aid for Scientific Research ((C) No. 20K04524).

Keiko Fukuda and Yamato Wakamatsu are with Tokyo Metropolitan College of Industrial Technology, 8-17-1 Minamisenjyu, Arakawaku, Tokyo 116-8523, Japan. Mamiko Fujii is with Sophia University, Tokyo Japan. (e-mail: fukuda@metro-cit.ac.jp).

$$b_i = \sum_j A_{i,j} x_j \,, \tag{4}$$

where x_j is expressed as $x_j = \frac{\delta \mu_{a,j}}{\mu_a}$. (5)

By creating a matrix of all of the observation data, $\boldsymbol{b}$, for all SD pairs and solving it for the elements of the absorption-coefficient perturbation, $\boldsymbol{x}$, as

$$\boldsymbol{b} = \boldsymbol{A}\boldsymbol{x} \,. \tag{6}$$

In the inverse problem, we adopted the Moore–Penrose inversion to estimate the elements of $\boldsymbol{x}$. The solution with regularized analysis $\boldsymbol{x}_R$ is given by

$$\boldsymbol{x}_R = (\boldsymbol{A}^T\boldsymbol{A} + \lambda \boldsymbol{I})^{-1}\boldsymbol{A}^T\boldsymbol{b}, \tag{7}$$

where $\boldsymbol{I}$ is the identity matrix and λ is the Tikhonov regularization parameter. We fixed λ by the L-curve method.

Then, the sensitivity matrix, $\boldsymbol{A}$, and a window matrix, $\boldsymbol{W}$, were applied to $\boldsymbol{x}_R$ to calculate the observation data after suppressing the superficial changes, $\boldsymbol{b}_R$:

$$\boldsymbol{b}_R = \boldsymbol{A}\boldsymbol{W}\boldsymbol{x}_R \,. \tag{8}$$

Here, $\boldsymbol{W}$ is an identity matrix with a part set to 0 to extract the changes in the target layer by masking the changes in the superficial layer. Then, $\boldsymbol{b}_R$ was solved using the observation data $\boldsymbol{b}$:

$$\boldsymbol{b}_R = \boldsymbol{A}\boldsymbol{W}(\boldsymbol{A}^T\boldsymbol{A} + \lambda \boldsymbol{I})^{-1}\boldsymbol{A}^T\boldsymbol{b} \,. \tag{9}$$

This solution was finally reconstructed into a two-dimensional space to obtain a topographic image.

III. Measurement Method

A. Experimental task

For evaluating the separation effect of hemodynamics by the depth-selective filter, we used the Stroop GO/NO-GO task [7] designed to estimate the response in the prefrontal cortex. Figure 1 shows the experimental procedure. Japanese red, blue, and white hiragana characters were presented in a random order. A GO/NO–GO task shows unmatched colored letters presented at approximately 60% frequency and a GO task shows letters presented in red Each task displayed 3 s with 3s interval. The subject pressed the button when the color letters did not match. Each stimulus appeared alternately 32 times. The average correct answer rate was 80 %.

B. Measurement system

The experiments were conducted using a prototype system (Electro-Design Corp.). A multi-modulated two-wavelength semiconductor lasers were used as the light sources. The detected change in the light absorption were demodulated with 5.6 Hz sampling frequency. In order to reduce high frequency noise, 1-Hz-LPF was applied. Then, the proposed depth-selective filter was applied. Furthermore, the change in the oxygenated hemoglobin concentration (OxyHb) and deoxygenated hemoglobin concentration (DeoxyHb) were calculated from the change in the light absorption according to the modified Beer-Lambert law. Then, for reducing noise and monitoring the response to according to the experimental task, 32 addition averaging of 18 s was applied.

For analyzing the signal characteristics, cross-correlation coefficient was used [9]. The cross-correlation coefficient of OxyHb between channels was used for estimating the hemodynamic change and the cross-correlation coefficient of OxyHb and DeoxyHb of the individual channel was used for estimating the brain activity.

The sensor arrangement is shown Fig. 2. Ten light sources and eight detectors are located in an area of 60 x 75 mm. The midpoint between the light source and the detector is considered the location of the topographical signal source. The normal SD signals measured at a distance of 30 mm are channels 1 to 24. The SSD signals measured at a distance of 15 mm distance are channels 25 to 30. The sensor holder was placed directly above the eyebrows, with a 0 mm position between the eyebrows.

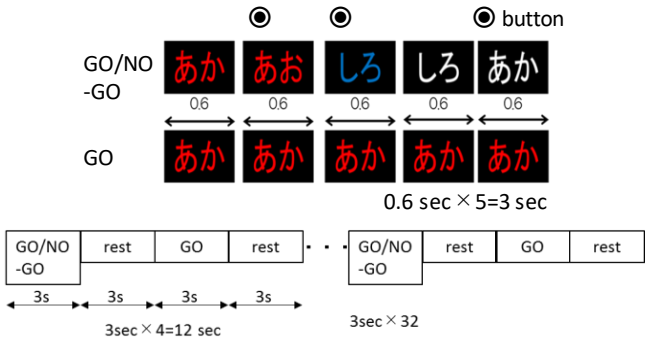

Figure 1. Configuration of the experimental task.

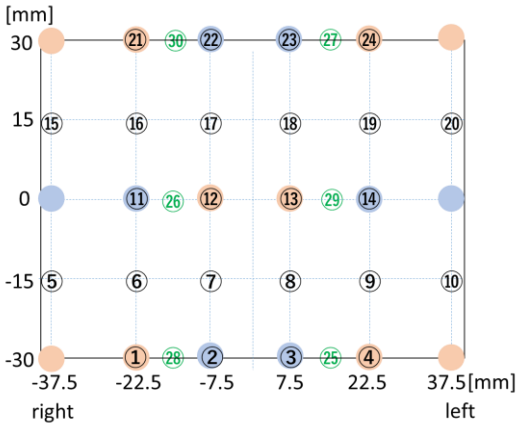

Figure 2. Sensor arrangement.
①-㉔: SD channel (30 mm) and ㉕-㉚: SSD channel (15mm).

IV. Measurement and Analysis

Written informed consent was obtained from 11 healthy subjects (males 20±0.5). Results were confirmed for 10 of the 11 subjects, excluding one with large noisy signal. The correct answer rate in the GONO-GO section of the experimental task ranged from 77 to 98.5%, with an average of 86.6%.

Therefore, it is considered to be appropriate as a task to promote brain activation.

An example of the temporal changes of oxygenated hemoglobin concentration (OxyHb) and the deoxygenated hemoglobin concentration (DoxyHb) after applying the LPF is shown in Fig. 3 (Subject I). Focusing on the OxyHb change, the SD signals including the brain functional response and the SSD signals mainly including the superficial hemodynamic change are similar. When the cross-correlation coefficient between the SD signal and SSD signal of OxyHb was calculated, 17 out of 24 channels showed a high correlation of 0.8 or more with the nearby SSD signal. Similarly, high correlation of 0.8 or more in an average of 77 % was shown when calculating the cross-correlation coefficient between the SD signal and SSD signal of OxyHb for 10 subjects. These observation show that the hemodynamic change is dominant in the measurement of the frontal region and the reduction of the hemodynamic change is required.

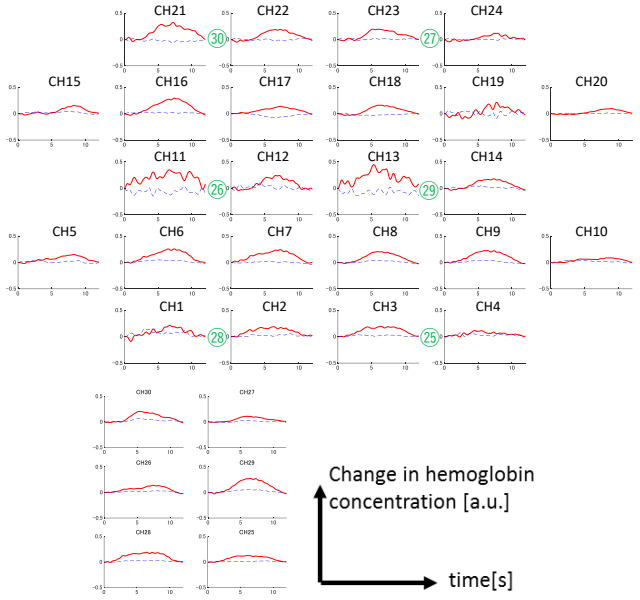

Figure 3. Change of oxygenated and the deoxygenated hemoglobin concentration (Subject I).

The temporal changes of OxyHb and DoxyHb after applying the depth-selective filter is shown in Fig. 4. When the oxygen required for brain activity is supplied to the capillaries of the brain tissue, a large influx of arterial blood simultaneously occurs and it leads to an increase in the oxygenated hemoglobin and a decrease in the deoxygenated hemoglobin. This tendency is observed in channels 11, 16 and 22. In these channels, the cross-correlation coefficient between OxyHb and DeoxyHb is -0.8 or less.

The spatial registration of NIRS channels is shown in Fig. 5. The spatial registration of NIRS channels can be projected to MNI space without MRI using 3D digitizer by NIRS-SPM [10]. According to the anatomical labeling for NIRS channels of this subject, channels 11, 16 and 22 are correspond to the frontopolar cortex that controls decision-making, and the dorsolaterdal prefrontal cortex that plans for complex cognitive behavior. These responses are considered to be reactions due to the Stroop GO/NO–GO task.

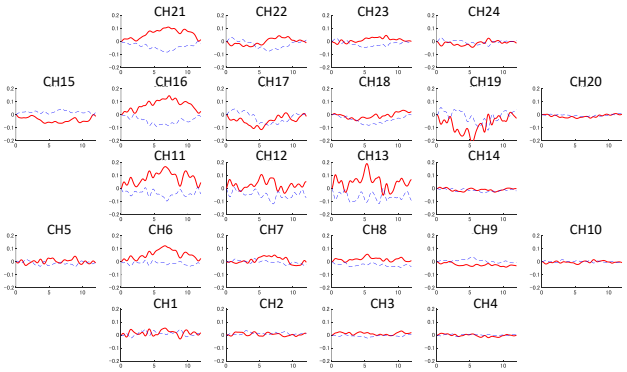

Figure 4. Change of oxygenated and the deoxygenated hemoglobin concentration after after applying the depth-selective filter (Subject I).

The spatial registration of NIRS channels is shown in Fig. 5. The spatial registration of NIRS channels can be projected to MNI space without MRI using 3D digitizer by NIRS-SPM [10]. According to the anatomical labeling for NIRS channels of this subject, channels 11, 16 and 22 are correspond to the frontopolar cortex that controls decision-making, and the dorsolaterdal prefrontal cortex that plans for complex cognitive behavior. These responses are considered to be reactions due to the Stroop GO/NO–GO task.

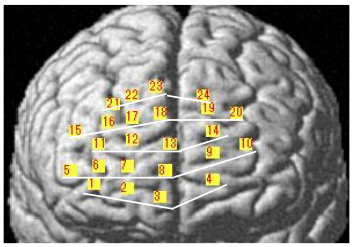

Figure 5. Sspatial registration of fNIRS channels (Subject I).

Another example of the temporal change in OxyHb and DeoxyHb before and after applying the depth-selective filters is shown in Fig. 6. In this subject, the hemodynamic change was smaller than that in the previous subject, and the pattern according to the brain activity (the increase of OxyHb and the decrease of DeoxyHb) were observed in channels 3 and 4 before applying the depth-selective filter. Also, unlike the previous case, the patterns showed two peaks corresponding to the GO/NO–GO task and the Go task. After applying the filter, the patterns similar to channels 3 and 4 were observed in several channels such as 2, 6 and 23. On the other hand, several channels (e.g. channel 10) showed an inverse trend of the patterns of OxyHb and DeoxyHb. It is considered that the change in blood flow dynamics is small so that the correction effect by the depth-selective filter was excessive.

The spatial registration of NIRS channels is shown in Fig. 7.The channels 3 and 4 correspond to the orbitofrontal area. It is considered that the response to receive information from the visual cortex, that is, the response to the presented visual stimulus was reflected.

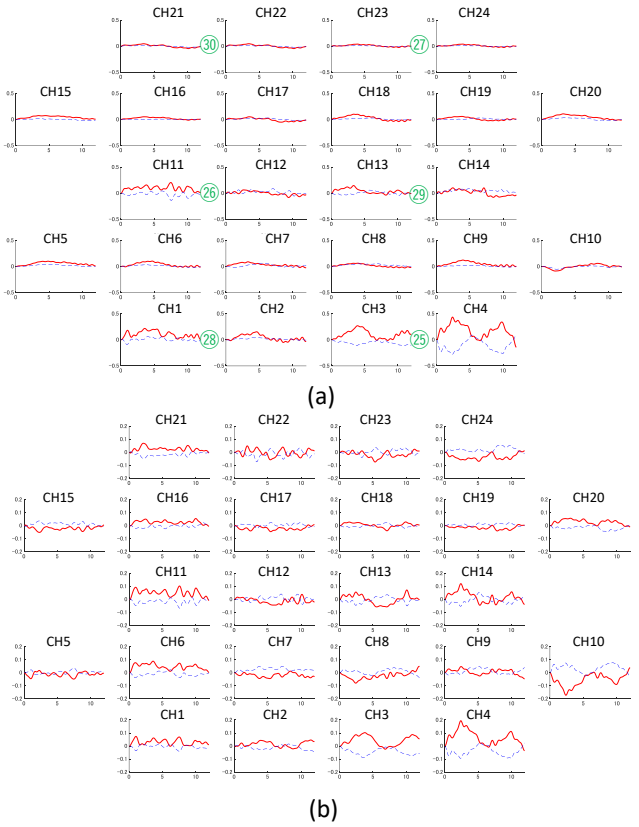

Figure 6. Change of oxygenated and the deoxygenated hemoglobin concentration (a) before and (b) after applying the depth-selective filters (Subject D).

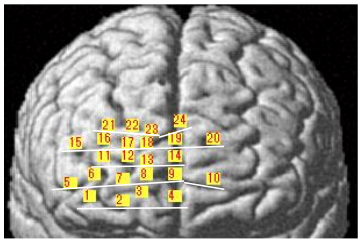

Figure 7. The spatial registration of fNIRS channels (Subject D).

The cross-correlation coefficient in each channel between OxyHb and DeoxyHb after applying the depth-selective filter are summarized in Fig. 8. The number of subjects with a coefficient of -0.8 or less are shown in below the channel number. Although the sensor arrangement varies by subject, 5 or more cases fall into the category in the channels in 11, 12, 13, 14, 15 and 21. It shows that many responsive channels on the right and upper area, and this is consistent with previous studies [11].

On the other hand, there are few channels with the coefficient of -0.8 or less in lower area of the forehead, while the change in OxyHb is large before applying the filter. This indicates that the hemodynamic change is dominant in this area and that the main response in this area is a reaction by a visual stimulus having two peaks as shown in Fig. 6.

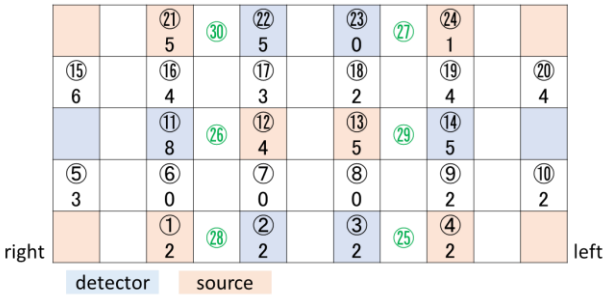

Figure 8. The cross-correlation coefficient with the depth-selective filter.

V. Conclusion

We applied the depth-selective filter to brain function measurement and showed the filter is effective in separating the hemodynamic change to acquire signals. The advantage of this method is that the number of SSD signal acquisition channels are less than that of the SD signals acquisition channels, and the arrangement with double density is not always necessary. Therefore, this method can be easily applied to the preprocessing for estimation of the brain activated region. We used the Stroop GO/NO–GO task to measure the brain function. Estimating from the position of the measured signal change, it is considered that the responses regarding the decision-making and the visual stimuli were obtained. Therefore, the Stroop GO/NO–GO task is useful for analyzing brain activity of the forehead area.

References

[1] A. Maki, Y. Yamashita, Y. Ito, E. Watanabe, Y. Mayanagi, and H. Koizumi, “Spatial and temporal analysis of human motor activity using noninvasive NIR topography,” Med. Phys., vol. 22, pp. 1997–2005, 1995.

[2] T.J. Huppert, R.D. Hoge, S.G. Diamond, M.A. Franceschini, and D.A. Boas, ”A temporal comparison of BOLD, ASL, and NIRS hemodynamic responses to motor stimuli in adult humans,” NeuroImage,vol.29, pp. 368 – 382, 2006.

[3] T. Yamada, S. Umeyama, K. Matsuda, “Separation of fNIRS Signals into Functional and Systemic Components Based on Differences in Hemodynamic Modalities,” PLOS ONE, vol.7, pp. e50271, 2012.

[4] T. Yamada, and S. Umeyama, “Multidistance probe arrangement to eliminate artifacts in functional near infrared spectroscopy,” J. Biomed. Opt., vol. 14, pp. 064034, 2009.

[5] A. Ishikawa, H. Udagawa, Y. Masuda, S. Kohno, T. Amita, and Y. Inoue, “Development of double density whole brain fNIRS with EEG system for brain machine interface,” IEEE EMBC, vol. 2011, pp. 6118–6122, 2011.

[6] M. Fujii, K. Nakayama, “Signal filtering algorithm for depth-selective diffuse optical topography,” Phys. Med. Biol. 54:1419-1433, 2009.

[7] Keiko Fukuda, Shun Seki, Ren Kunii, Li-qun Wang, Keita Tanaka and Shinya Kuriki, “Experimental tasks using fMRI measurement for evaluating NIRS signal characteristics,“ IEEE EMBC, WePOS-32.31, 2019.

[8] A. Ishimaru, “Wave propagation and scattering in random media,” IEEE Press, 341–343, 1999.

[9] K. Fukuda, H. Takemoto, and A. Ikeda, “Analytical approach to the temporal changes in NIRS signals to separate hemodynamic change from brain activity,” IEEE EMBC, vol.2o16, pp.1393-1396, 2016.

[10] Ye, J. C., Tak, S., Jang, K. E., Jung, J., Jang, J., 2009, NIRS-SPM: Statistical parametric mapping for near-infrared spectroscopy. NeuroImage 44, 428-447.

[11] Chikazoe, K. Jimura, T. Asari, K. Yamashita, H. Morimoto, S.Hirose, Y. Miyashita and S. Konishi, Cerebral Cortex an.19:pp.146–152,2009.